Received: 28 January 2022 | Revised: 17 March 2022 | Accepted: 11 April 2022

IET Signal Processing

DOI: 10.1049/sil2.12131

The Institution of Engineering and Technology WILEY

ORIGINAL RESEARCH

Towards 6G: Spectrally efficient joint radar and communication with radio frequency selection, interference and hardware impairments (invited paper)

Aryan Kaushik[1] | Evangelos Vlachos[2] | John Thompson[3] | Maziar Nekovee[1] | Fraser Coutts[3]

[1]6G Lab, School of Engineering and Informatics, University of Sussex, Brighton, UK

[2]Industrial Systems Institute, Athena Research and Innovation Centre, Marousi, Greece

[3]Institute for Digital Communications, The University of Edinburgh, Edinburgh, UK

Correspondence

Aryan Kaushik, 6G Lab, School of Engineering and Informatics, University of Sussex, Brighton, UK.
Email: aryan.kaushik@sussex.ac.uk

Funding information

Engineering and Physical Sciences Research Council, Grant/Award Number: EP/S000631/1

Abstract

The joint radar-communication (JRC) system is envisioned as an emerging sixth generation (6G) technology to tackle spectral congestion and hardware limitations by jointly implementing the communication and radar sensing on the same hardware platform and using the common radio frequency (RF) resources. Joint radar-communication systems with a multi-antenna setup leads to higher degrees of freedom, and hybrid beamforming can be exploited to achieve lower hardware complexity than conventional fully digital systems. This paper aims to design a spectral efficiency maximisation approach for a 6G inclined JRC system with hybrid beamforming and multi-antenna setup while considering the interference between communication and radar operations and hardware impairments in the system. The rate expressions for communication and radar operations are defined, and the joint spectral efficiency is maximised via optimising the number of RF chains using an efficient selection algorithm taking into account the interference of one operation to the other and system hardware distortion. The simulation results are shown to support the effectiveness of the proposed approach, and they are compared with that of existing fully digital and hybrid beamforming based baseline methods with fixed number of RF chains. The proposed approach also exhibits a desirable communication-radar trade-off in terms of spectral efficiency gains.

KEYWORDS

5G mobile communication, MIMO communication, MIMO radar, precoding

1 | INTRODUCTION

The existing sub 6 GHz frequency spectrum is expected to become very congested in the fifth generation (5G) era due to the increasing user demand for mobile communications. As per the Cisco report [1], there will be over 70% mobile users of the world population by 2023 with 13.1 billion global mobile devices, two-thirds of global population with internet access, and 4 billion networked devices/connections just in Western Europe. The Ericsson mobility report [2] forecasts a high increase in mobile data traffic such as the global monthly average usage to be 41 GB per smartphone and 51 GB in Western Europe by 2027. Current technology advancements in the 5G systems are in commercial use and their constant growth will lead to 4.4 billion subscriptions with 5G services constituting towards 83% of all subscriptions in Western Europe by 2027 [2]. This high data traffic and enhanced demands for advanced technology lead us to seek for more available spectral resources or sharing the ones used for other applications and systems such as radar technology. The 5G Americas white paper [3] suggests that achieving high data rates and long-term spectrum planning and harnessing are envisioned to be one of the

fundamental technologies in the sixth generation (6G) mobile communications. In terms of spectrum sharing, the available radar spectrum can be made available for sharing between the radar functionality and the wireless communication systems [4].

The integrated sensing and communication (ISAC) technology envisioned for 6G can benefit from sharing of the spectral and hardware resources in order to communicate with downlink users and simultaneously detect radar targets [5]. Radar systems have tremendous benefits in terms of detecting targets, determining distance and velocity, and movement tracking using radio waves. Incorporating communication modelling with radar signalling provides multiple benefits in terms of functionality and applications over these individual systems. We can infer that the ISAC technology enhances the range of functions for these existing systems many fold and provides robust 6G solution to spectral congestion and hardware inefficiency issues. Furthermore, ISAC systems hold advanced aerial, vehicular, military, electronic warfare and internet-of-things (IoT) applications [6, 7]. For instance, the advanced airborne and shipborne radio frequency (RF) systems with communication, radar and electronic warfare applications have been developed to support jointly multiple functionalities, such as in Ref. [8]. The continuous-wave radar requires significant isolation between the transmitter (TX) and the user equipment (UE) to continuously transmit the signal and receive the radar echo, while the pulsed radar operating in a time-division manner, which can be used for transmitting dual functional waveforms. Also orthogonal frequency division multiplexing signals can be employed for radar and communication systems in order to co-design the radio sensing and communication functions [9].

Beyond spectral-coexistence systems, where a coordination or central unit for exchanging information between radar and communication systems is required, the joint radar-communication (JRC) systems integrate the complete hardware platform and the transmitted signal waveform of the two systems. That is they perform simultaneous target detection and information communication by using the same hardware and signal for both operations. The existing ISAC systems can be categorised into the following [10]: (a) communication-centric, where radar sensing is the secondary function of a communication system; (b) radar-centric, where information communication is the secondary function of a radar system; and (c) joint systems, which are capable of tuning the performance trade-off between both operations.

Such JRC systems, by sharing the functionalities of radar sensing and information communication on a single hardware, reduce the overall power consumption, system size and information exchange latency. However, advanced signal processing strategies are required to truly realise the benefits and improve trade-off scenarios. For instance, the information embedding of radar waveform with communication signals also demands advanced modulation approaches such as in Ref. [11], which exploits antenna and frequency agility for enhanced performance. For convergence towards a truly efficient JRC design, we need to consider the impact of hardware distortion parameters and interference originating from the two simultaneous operations.

As a widely researched and promising technology for the next generation systems, high frequency millimetre wave (mmWave) frequencies above 28–30 GHz range can be deployed for JRC systems. MmWave spectrum modelling has been implemented in recent beamforming techniques to realise energy and spectral efficient communications [12, 13]. Furthermore, with few multipath components in the mmWave band, radar echo may experience less clutter interference in comparison to the sub-6 GHz bands [14]. It is expected that mmWave technology will equip favourable sensing functionality, which may be applied to vehicular communication scenarios [15, 16], for example, 77 GHz will be used for automative radar in driverless cars. Note that the proposed method in this paper is general and can be applied to different carrier frequencies such as the sub-6 GHz and terahertz bands. The multiple-input multiple-output (MIMO) antenna setup-based radar and communication systems with multiple radar and communication users provide high degrees of freedom and can reduce large path loss values at such high frequency bands [17–19].

The conventional digital precoding architecture, with one RF chain and associated digital-to-analogue converters (DACs) at each antenna, to implement wide bandwidths and large scale antennas in JRC systems leads to a high hardware complexity and cost inefficiency. Most of the existing literature such as Ref. [18–20] implements fully digital precoding in MIMO JRC systems. There has been recent advances in terms of lowering the hardware complexity and designing dual functional waveforms for JRC by using analogue components [21]. However, further research is required in this direction, which exploits low hardware complexity architectures for JRC systems. Hybrid precoding, which implements fewer RF chains than the number of transmit antennas can be a cost efficient alternative for large scale antenna systems [22–24].

The RF chains consume considerable power, which reduces the cost efficiency of the communication system. In order for the hardware to perform simultaneous sensing and communication functions, it is very important to regulate the use of RF chains in order to save power consumption. Thus for JRC systems, as the RF chain components are highly power consuming, optimising the number of RF chains to achieve a low hardware complexity solution is important. Such solutions have been recently presented in order to design energy and hardware efficient JRC systems via RF chain selection [25]. Implementing high speed analogue-to-digital converters (ADCs) can further increase the performance of JRC systems [17]; however, high resolution sampling would considerably increase the hardware complexity [26]. In the literature, low resolution ADCs have been implemented with hybrid beamforming such as for efficient channel estimation [27]. Regulating the high analogue-to-digital converter resolution sampling requirements can lead to a low hardware complexity and energy efficient system [28]. Ref. [29] benefits from the low resolution ADCs in the JRC systems; however, hardware inefficient digital precoding architecture is considered.

An energy efficient RF chain and DAC-bit selection approach is provided in Ref. [30]; however, only the equal bit allocation and MIMO communication-only scenario is addressed. Ref. [31] provides an advanced approach to optimise varying DAC bit resolution for such systems in order to achieve an energy efficient and low hardware complexity solution. In the context of MIMO JRC systems, the recent literature such as in Ref. [32] suggests the use of low resolution DACs with rate splitting multiple access for interference mitigation; however, selecting the optimal number of RF chains has not been addressed, which is crucial for reduction of the power consumption. Ref. [33] discusses the use of low resolution DACs and RF chain selection with hybrid beamforming; however, there are no practical hardware impairments and impact of interference is also not considered in the JRC system design. Due to the co-design of radar sensing and communication functions, imperfect hardware architectures to address practical implementations and interference of one operation on the other are of paramount importance in terms of JRC system design. The low hardware complexity architectures using hybrid beamforming are also required to exhibit high spectral efficiency for a truly efficient JRC system.

In a nutshell, the work on developing spectral efficient RF selection approach for MIMO JRC systems with hybrid precoding, taking into account interference between radar and communication operations and hardware impairments, has not been addressed in the literature. We formulate a spectral efficiency maximisation problem, where the effect of the interference on both the radar and communications performance are considered when hardware impairment errors are also introduced. The optimisation problems consider communication and radar-specific constraints to achieve best possible performance in terms of both sensing and communication operations. An RF chain selection procedure for the hybrid beamforming-based MIMO JRC system is proposed, which activates or deactivates the number of RF chains based on the optimal solution to the difficult rate maximisation problem.

The main contributions of this paper can be listed as follows:

- This paper introduces an interference-oriented and practical hardware impairment-based spectral efficiency maximisation problem for the joint radar and communication functions taking into account the radar mutual information and the communication rate. The impact of hardware impairment error and interference of one operation to the other are taken into account.
- We develop a selection procedure for JRC systems to optimise the number of RF chains by activating only the required number of RF chains. The RF selection procedure maximises the spectral efficiency for both communication and radar operations. Furthermore, it saves hardware complexity and can achieve an overall spectral and hardware efficient design for JRC systems to be deployed in the 6G communication standards.
- The effectiveness of the proposed method is investigated through extensive numerical results. These show that the proposed method with radar interference and hardware impairments achieves high spectral efficiency when compared with the existing fully digital and hybrid beamforming method with fixed number of RF chains. A favourable communication and radar trade-off in terms of spectral efficiency gains via proposed approach is also observed.

Notation and Organisation: A summary of notation used throughout this paper has been listed in Table 1. In terms of the paper organisation, Section 2 presents the system model including communication and radar models, which define the communication channel, and the dual functional signal with hardware impairments and interference terms. Sections 3 presents the problem formulation for the RF chain selection, and the solution to obtain a spectrally efficient hybrid precoding-based JRC system. Section 4 verifies the effectiveness of the proposed technique through numerical results. Section 5 concludes the outcomes of the proposed work in this paper.

2 | SYSTEM MODEL

We consider a MIMO JRC system with N_{T} antennas at the TX communicating with N_{R} antennas at the UE. The number of targets for the radar sensing operation are denoted as N_{p}. We consider a hybrid beamforming architecture for the MIMO JRC system, so there are fewer available RF chains, L_{T}, than

TABLE 1 Summary of notation

Notation	Term
$\mathbf{A}$	Matrix variable
$\mathbf{a}$	Vector variable
a	Scalar variable
$\mathbf{A}^T$	Matrix transpose of $\mathbf{A}$
$\mathbf{A}^H$	Complex conjugate transpose of $\mathbf{A}$
$\|\mathbf{A}\|_F$	Frobenius norm of $\mathbf{A}$
$\|\mathbf{a}\|_2$	L2 norm of the vector $\mathbf{a}$
$\mathrm{tr}(\mathbf{A})$	Trace of matrix $\mathbf{A}$
$\|\mathbf{A}\|$	Determinant of matrix $\mathbf{A}$
$[\mathbf{A}]_{i,j}$	Matrix element at the i-th row and j-th column
$\mathbf{a}_i$	The i-th element of vector $\mathbf{a}$
$\mathbf{I}_N$	$N \times N$ identity matrix
$\mathbf{I}_{N\times K}$	Column concatenated matrix $[\mathbf{I}_N\ \mathbf{0}_{N\times K}]$
$\times$	Scalar multiplication
$\mathbb{E}$	Expectation operator
$\mathbb{C}^{X\times Y}$	Set of $X \times Y$ size matrix with complex entries
$\mathbb{R}^{X\times Y}$	Set of $X \times Y$ size matrix with real entries
$\mathcal{CN}(a,b)$	Complex Gaussian vector with mean a, variance b

the number of the TX antennas, that is, $1 \leq L_{\mathrm{T}} \leq N_{\mathrm{T}}$. The transmit symbol signal $\mathbf{s} \in \mathbb{C}^{N_{\mathrm{R}} \times 1}$ satisfies the condition of $\mathbb{E}\{\mathbf{s}\mathbf{s}^{H}\} = \mathbf{I}_{N_{\mathrm{R}}}$. Note that the symbol signal comprises both the communication and radar vector terms, that is, $\mathbf{s}_{\mathrm{com}} \in \mathbb{C}^{\frac{N_{\mathrm{R}}}{2} \times 1}$ and $\mathbf{s}_{\mathrm{rad}} \in \mathbb{C}^{\frac{N_{\mathrm{R}}}{2} \times 1}$ referring to the communication and radar operations, respectively, with $\mathbf{s} = \begin{bmatrix} \mathbf{s}_{\mathrm{com}}^{T} & \mathbf{s}_{\mathrm{rad}}^{T} \end{bmatrix}^{T}$.

Following Figure 1, the hybrid precoding implementation in the MIMO JRC system can be observed, which shows individual blocks representing, respectively, the communication and radar operations. In the system model, the digital precoder matrix is denoted by $\mathbf{F}_{\mathrm{BB}}$, which is followed by the RF Chain and DAC setup. The analogue precoder $\widehat{\mathbf{F}}_{\mathrm{RF}}$ is implemented via a phase shifting network, which consists of $f_i \in \mathbb{C}^{\frac{N_{\mathrm{T}}}{L_{\mathrm{T}}} \times 1}, \forall i = 1, \ldots, L_{\mathrm{T}}$ elements, with constant-modulus entries. The hybrid precoder decomposition $\mathbf{F}_{\mathrm{BB}}^{\mathrm{com}} \widehat{\mathbf{F}}_{\mathrm{RF}}^{\mathrm{com}}$ accounts for the digital and RF precoding during communication operation, and similarly, $\mathbf{F}_{\mathrm{BB}}^{\mathrm{rad}} \widehat{\mathbf{F}}_{\mathrm{RF}}^{\mathrm{rad}}$ accounts for the digital and RF precoding during radar operation. Figure 1 also shows the *selection method* as a framework, which drives the selection of optimal number of RF chains when communication and radar sensing operations are taking place in the MIMO JRC system.

In terms of the dual function transmitted signal for hybrid precoder, $\mathbf{x}_{\mathrm{H}}$ can be expressed as

$$\mathbf{x}_{\mathrm{H}} = \widehat{\mathbf{F}}_{\mathrm{RF}}^{\mathrm{com}} \mathbf{F}_{\mathrm{BB}}^{\mathrm{com}} \mathbf{s}_{\mathrm{com}} + \widehat{\mathbf{F}}_{\mathrm{RF}}^{\mathrm{rad}} \mathbf{F}_{\mathrm{BB}}^{\mathrm{rad}} \mathbf{s}_{\mathrm{rad}} + \underbrace{\widehat{\mathbf{F}}_{\mathrm{RF}}^{\mathrm{com}} \mathbf{F}_{\mathrm{BB}}^{\mathrm{rad}} \mathbf{s}_{\mathrm{rad}} + \widehat{\mathbf{F}}_{\mathrm{RF}}^{\mathrm{rad}} \mathbf{F}_{\mathrm{BB}}^{\mathrm{com}} \mathbf{s}_{\mathrm{com}}}_{\text{interference term}}, \tag{1}$$

where the *interference term* indicates the interference at the TX from radar and communication operations to each other. For the dual functional transmission, the corresponding communication and radar symbol signals follows $\|\mathbf{s}_{\mathrm{com}}\|^2 = \|\mathbf{s}_{\mathrm{rad}}\|^2 = 1$.

In order to communicate the information, the narrowband modelled mmWave channel $\mathbf{H}_{\mathrm{com}} \in \mathbb{C}^{N_{\mathrm{R}} \times N_{\mathrm{T}}}$ can be expressed as

$$\mathbf{H}_{\mathrm{com}} = \sqrt{\frac{N_{\mathrm{T}} N_{\mathrm{R}}}{N_{\mathrm{m}}}} \sum_{l=1}^{N_{\mathrm{m}}} \alpha_l \mathbf{a}_{\mathrm{R}}\left(\phi_l^r\right) \mathbf{a}_{\mathrm{T}}^{H}\left(\phi_l^t\right), \tag{2}$$

where N_{m} denotes the number of multipaths, α_l is the gain of l-th path, and $\mathbf{a}_{\mathrm{T}}\left(\phi_l^t\right) = \frac{1}{\sqrt{N_T}}\left[1, e^{j\frac{2\pi}{\lambda} d \sin\left(\phi_l^t\right)}, \ldots, e^{j(N_T-1)\frac{2\pi}{\lambda} d \sin\left(\phi_l^t\right)}\right]^{T}$ is the transmit steering vector with ϕ_l^t as the angle of departure, d the antenna spacing and λ the wavelength. The beam steering vector follows a uniform linear array setup, and the proposed approach also be applied with antenna setups such as circular array and rectangular array. Similarly, $\mathbf{a}_{\mathrm{R}}\left(\phi_l^r\right)$ denotes the receive array response vector with ϕ_l^r as the angle of arrival. The radar channel is denoted as $\mathbf{H}_{\mathrm{rad}}$, which is unknown; however, the channel covariance matrix $\mathbf{R}_{\mathrm{T}}$ related to the columns of channel is known. We assume that perfect channel state information of the communication channel $\mathbf{H}_{\mathrm{com}}$ is available at the TX and the UE.

The corresponding communication received signal at the UE can be expressed as

$$\begin{aligned} y_{\mathrm{com}} &= \mathbf{w}_{\mathrm{com}}^{H} \mathbf{H}_{\mathrm{com}} \mathbf{x}_{\mathrm{H}} + n_{\mathrm{com}} \\ &= \mathbf{w}_{\mathrm{com}}^{H} \mathbf{H}_{\mathrm{com}} \widehat{\mathbf{F}}_{\mathrm{RF}}^{\mathrm{com}} \mathbf{F}_{\mathrm{BB}}^{\mathrm{com}} \mathbf{s}_{\mathrm{com}} \\ &\quad + \underbrace{\mathbf{w}_{\mathrm{com}}^{H} \mathbf{H}_{\mathrm{com}} \left(\widehat{\mathbf{F}}_{\mathrm{RF}}^{\mathrm{rad}} \mathbf{F}_{\mathrm{BB}}^{\mathrm{rad}} \mathbf{s}_{\mathrm{rad}} + \widehat{\mathbf{F}}_{\mathrm{RF}}^{\mathrm{com}} \mathbf{F}_{\mathrm{BB}}^{\mathrm{rad}} \mathbf{s}_{\mathrm{rad}} + \widehat{\mathbf{F}}_{\mathrm{RF}}^{\mathrm{rad}} \mathbf{F}_{\mathrm{BB}}^{\mathrm{com}} \mathbf{s}_{\mathrm{com}}\right)}_{\gamma_{\mathrm{rad-com}}} + n_c, \end{aligned} \tag{3}$$

where $\mathbf{w}_{\mathrm{com}}$ is the combiner vector for the communication part of the TX signal, n_c is the independent and identically distributed (i.i.d.) complex additive white Gaussian noise (AWGN) while communication operation takes place, with $n_c \sim \mathcal{CN}\left(0, \sigma_n^2\right)$. In Equation (3), the term $\gamma_{\mathrm{rad-com}}$ represents the interference at the UE for communication operation.

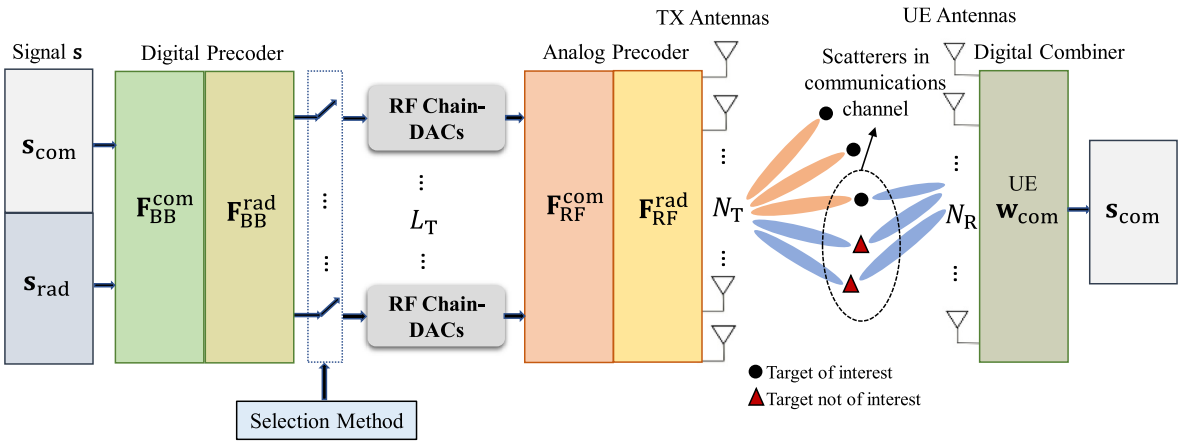

FIGURE 1 A multiple-input multiple-output (MIMO) joint radar-communication (JRC) system with hybrid precoding and radio frequency (RF) selection framework

Similarly, the corresponding radar received signal at the TX is expressed as

$$\begin{aligned} y_{\text{rad}} &= \mathbf{w}_{\text{rad}}^H \mathbf{H}_{\text{rad}} \mathbf{x}_{\text{H}} + n_{\text{rad}} \\ &= \mathbf{w}_{\text{rad}}^H \mathbf{H}_{\text{rad}} \widehat{\mathbf{F}}_{\text{RF}}^{\text{rad}} \mathbf{F}_{\text{BB}}^{\text{rad}} \mathbf{s}_{\text{rad}} \\ &\quad + \underbrace{\mathbf{w}_{\text{rad}}^H \mathbf{H}_{\text{rad}} \left(\widehat{\mathbf{F}}_{\text{RF}}^{\text{com}} \mathbf{F}_{\text{BB}}^{\text{com}} \mathbf{s}_{\text{com}} + \widehat{\mathbf{F}}_{\text{RF}}^{\text{com}} \mathbf{F}_{\text{BB}}^{\text{rad}} \mathbf{s}_{\text{rad}} + \widehat{\mathbf{F}}_{\text{RF}}^{\text{rad}} \mathbf{F}_{\text{BB}}^{\text{com}} \mathbf{s}_{\text{com}} \right)}_{\gamma_{\text{com-rad}}} + n_r, \end{aligned} \tag{4}$$

where $\mathbf{w}_{\text{rad}}$ is the combiner for the radar part of the TX signal, n_r corresponds to the AWGN term when radar operation takes place, with $n_c \sim \mathcal{CN}(0, \sigma_n^2)$. Note that $\mathbf{w}_{\text{rad}}$ accounts for the radar echo signal processing at the TX. In Equation (4), the term $\gamma_{\text{com-rad}}$ represents the interference at the UE for radar sensing operation.

In this work, we also consider hardware imperfections that may arise from one or more sources [34], such as Phase Noise, Mutual Coupling, RF Hardware Imperfections, and Beam Squint [13]. To model their effect, we adopt the following decomposition:

$$\widehat{\mathbf{F}}_{\text{RF}} = \mathbf{F}_{\text{RF}} + \mathbf{\Phi}, \tag{5}$$

where $\mathbf{F}_{\text{RF}}$ is the ideal analogue beamformer for the communication operation, and $\mathbf{\Phi}$ is the noise matrix that captures hardware imperfections in the analogue circuitry. We have a similar expression for the radar analogue beamformer.

In addition to designing the optimal precoder matrices, the aim of the dual function JRC system is to obtain a transmit beampattern that points to the targets of interest. For each for the N_{p} targets located at angles ϕ_i, with $i = 1, \ldots, N_{\text{p}}$, the transmit beampattern of the radar can be expressed as

$$B_{\text{T}}(\phi_i) = \mathbf{a}_{\text{T}}^H(\phi_i) \mathbf{R}_{\text{T}} \mathbf{a}_{\text{T}}(\phi_i), \tag{6}$$

where $\mathbf{R}_{\text{T}} \in \mathbb{C}^{N_{\text{p}} \times N_{\text{p}}}$ being the covariance matrix of the transmit signal. Designing the transmit radar beampattern $B_{\text{T}}(\phi_i)$, in Equation (6), is equivalent to designing the transmit covariance matrix $\mathbf{R}_{\text{T}}$, which is a function of the hybrid precoding matrices, that is, $\mathbf{R}_{\text{T}} = \mathbf{F}_{\text{RF}} \mathbf{F}_{\text{BB}} (\mathbf{F}_{\text{RF}} \mathbf{F}_{\text{BB}})^H$, where $\mathbf{F}_{\text{RF}}$, $\mathbf{F}_{\text{BB}}$ matrices consist of the digital/analogue communication and radar components as described above. The sub-arrayed MIMO radar beamformer and the diagonal elements of the optimal radar precoder $\mathbf{F}_{\text{rad}}^{\text{opt}}$ consist of $\mathbf{v}_{\text{i}} \in \mathbb{C}^{\frac{N_{\text{t}}}{N_{\text{p}}} \times 1}$ elements, which are composed by the entries of $\mathbf{a}_{\text{T}}(\phi_i)$ $\forall i = 1, \ldots, N_{\text{p}}$, located at the corresponding slots. The radar covariance matrix associated with $\mathbf{F}_{\text{rad}}^{\text{opt}}$ is $\mathbf{R}_{\text{T}}^{\text{opt}} = \mathbf{F}_{\text{rad}}^{\text{opt}} \left(\mathbf{F}_{\text{rad}}^{\text{opt}} \right)^H$, which corresponds to a well-designed and optimal radar beampattern. Next, we discuss the spectral efficiency maximisation via RF chain selection for the MIMO JRC system with hybrid beamforming architecture.

3 | SPECTRAL EFFICIENCY MAXIMISATION

In this section, we describe the rate expressions for both communications and radar operations while considering hybrid beamforming at the TX, formulate the spectral efficiency maximisation problem and present our proposed approach to select the optimal number of RF chains in an efficient manner for the MIMO JRC system with hybrid beamforming architecture.

3.1 | Problem formulation

The information rate for the communications operation can be expressed as

$$\begin{aligned} R_{\text{com}} = \log_2 \Bigg(1 + \frac{1}{\sigma_{\text{rad-com}}^2 + \zeta_{\text{com}}^2} \mathbf{w}_{\text{com}}^H \mathbf{H}_{\text{com}} \mathbf{F}_{\text{RF}}^{\text{com}} \mathbf{F}_{\text{BB}}^{\text{com}} \\ \times \mathbf{F}_{\text{BB}}^{\text{com}H} \mathbf{F}_{\text{RF}}^{\text{com}H} \mathbf{H}_{\text{com}}^H \mathbf{w}_{\text{com}} \Bigg), \end{aligned} \tag{7}$$

where the terms $\sigma_{\text{rad-com}}^2$ and ζ_{com}^2 correspond to the radar interference and hardware distortion during the communications operation, respectively. The information rate maximisation is given by:

$$\max_{\mathbf{F}_{\text{RF}}^{\text{com}} \mathbf{F}_{\text{BB}}^{\text{com}}} R_{\text{com}} \text{s.t.} \quad \text{tr}\left(\mathbf{F}_{\text{RF}}^{\text{com}} \mathbf{F}_{\text{BB}}^{\text{com}} \mathbf{F}_{\text{BB}}^{\text{com}H} \mathbf{F}_{\text{RF}}^{\text{com}H} \right) \leq P_{\text{max}}^{\text{com}} \tag{8}$$

where $P_{\text{max}}^{\text{com}}$ represents the maximum power budget terms for communication. Following Ref. [35] for instance, which describes the waveform design using the radar mutual information between the target reflections and target responses, we can similarly express the information rate for the radar operation as

$$\begin{aligned} R_{\text{rad}} = \log_2 \Bigg(1 + \frac{1}{\sigma_{\text{com-rad}}^2 + \zeta_{\text{rad}}^2} \mathbf{w}_{\text{rad}}^H \mathbf{H}_{\text{rad}} \mathbf{F}_{\text{RF}}^{\text{rad}} \mathbf{F}_{\text{BB}}^{\text{rad}} \\ \times \mathbf{F}_{\text{BB}}^{\text{rad}H} \mathbf{F}_{\text{RF}}^{\text{rad}H} \mathbf{H}_{\text{rad}}^H \mathbf{w}_{\text{rad}} \Bigg), \end{aligned} \tag{9}$$

where the terms $\sigma_{\text{com-rad}}^2$ and ζ_{rad}^2 correspond to the communications interference and hardware distortion during the radar operation, respectively. In the literature, the radar mutual information has been described to evaluate the radar performance, such as in Ref. [36, 37] where mutual information between target impulse response and echo/reflected signal is taken into account, provided there is prior knowledge of the dual function transmit signal (in the case of JRC) or radar-only transmit signal. Furthermore, in the case of JRC systems of Ref. [38], the radar mutual information is considered between the signal and target impulse response of radar and communication signals, while assuming that both radar and

communication signals partly have common information on the target. In this paper, as shown in Equation (9), we consider the radar rate consisting of the TX and UE beamforming parameters and channel term during radar operation of the JRC system taking into account the interference from communication operation and hardware distortion in the JRC system. The resulting radar rate maximisation is given by:

$$\max_{\mathbf{F}_{\mathrm{RF}}^{\mathrm{rad}}\mathbf{F}_{\mathrm{BB}}^{\mathrm{rad}}} R_{\mathrm{rad}} \text{s.t.} \quad \mathrm{tr}\left(\mathbf{F}_{\mathrm{RF}}^{\mathrm{rad}}\mathbf{F}_{\mathrm{BB}}^{\mathrm{rad}}\mathbf{F}_{\mathrm{BB}}^{\mathrm{rad}H}\mathbf{F}_{\mathrm{RF}}^{\mathrm{rad}H}\right) \leq P_{\max}^{\mathrm{rad}} \tag{10}$$

where $P_{\max}^{\mathrm{rad}}$ represents the maximum power budget terms for radar operation. Maximising the expression in Equation (10)with power constraint corresponds to the radar rate maximisation while the radar operation of target detection takes place.

The rate maximisation problems can be formulated as a sparse subset selection ones, by introducing a sparse RF chain selection diagonal matrix. For example, $\mathbf{S}^{\mathrm{com}}$ is the diagonal selection matrix for communication operation with diagonal entries from the set {0, 1}. Then, the hybrid beamformer for communication operation with $\mathbf{S}^{\mathrm{com}}$ selection matrix is expressed as

$$\mathbf{F}^{\mathrm{com}} = \mathbf{F}_{\mathrm{RF}}^{\mathrm{com}}\mathbf{S}^{\mathrm{com}}\mathbf{F}_{\mathrm{BB}}^{\mathrm{com}}, \tag{11}$$

and similarly, diagonal matrix $\mathbf{S}^{\mathrm{rad}}$ is used for RF chain selection procedure in the radar operation. Note that for brevity in the following, we drop the super index for the selection matrix and use $\mathbf{S}$ for both communications and radar operations.

Then, the information rate expression is given by:

$$R_{\mathrm{com}}(\mathbf{S}) = \log_2\left(1 + \frac{1}{\sigma_{\mathrm{rad-com}}^2 + \zeta_{\mathrm{com}}^2}\mathbf{w}_{\mathrm{com}}^H\mathbf{H}_{\mathrm{com}}\mathbf{F}_{\mathrm{RF}}^{\mathrm{com}}\mathbf{S}\mathbf{F}_{\mathrm{BB}}^{\mathrm{com}} \times \mathbf{F}_{\mathrm{BB}}^{\mathrm{com}H}\mathbf{S}\mathbf{F}_{\mathrm{RF}}^{\mathrm{com}H}\mathbf{H}_{\mathrm{com}}^H\mathbf{w}_{\mathrm{com}}\right) \tag{12}$$

and similarly for the radar rate $R_{\mathrm{rad}}(\mathbf{S})$, it can be expressed as

$$R_{\mathrm{rad}}(\mathbf{S}) = \log_2\left(1 + \frac{1}{\sigma_{\mathrm{com-rad}}^2 + \zeta_{\mathrm{rad}}^2}\mathbf{w}_{\mathrm{rad}}^H\mathbf{H}_{\mathrm{rad}}\mathbf{F}_{\mathrm{RF}}^{\mathrm{rad}}\mathbf{S}\mathbf{F}_{\mathrm{BB}}^{\mathrm{rad}} \times \mathbf{F}_{\mathrm{BB}}^{\mathrm{rad}H}\mathbf{S}\mathbf{F}_{\mathrm{RF}}^{\mathrm{rad}H}\mathbf{H}_{\mathrm{rad}}^H\mathbf{w}_{\mathrm{rad}}\right). \tag{13}$$

Algorithm 1 Proposed RF Selection for Communication Operation

Input: $\mathbf{H}_{\mathrm{com}}$, $\mathbf{H}_{\mathrm{rad}}$
Output: Diagonal binary matrix $\mathbf{S}^{(I_{\max})}$
Set $\kappa^{(0)} = 1$.
for $i = 1, 2, \ldots, I_{\max}$ **do**
  Use CVX [41] to solve $\max_{\mathbf{S}} \left\{\rho_{\mathrm{com}}(\mathbf{S}) - \kappa^{(i-1)}\sigma_{\mathrm{rad-com}}^2(\mathbf{S})\right\}$ s.t. $[\mathbf{S}]_{k,k} \in [0,1]$
  where R_{com} is approximated using Equation (14), and $\sigma_{\mathrm{rad-com}}^2$ is given in Equation (17).
  Approximate $R_{\mathrm{com}}(\mathbf{S}^{(i)})$ via Equation (14).
  Calculate the interference term $\sigma_{\mathrm{rad-com}}^2(\mathbf{S}^{(i)})$ in Equation (17).
  Compute $\kappa^{(i)} = \rho_{\mathrm{com}}(\mathbf{S}^{(i)})/\sigma_{\mathrm{rad-com}}^2(\mathbf{S}^{(i)})$.
end for

For medium and high impairment and interference noise, it is expected that the approximation $\log_2(1 + x) \approx x$ holds true. Thus, let us approximate the R_{com} expression as:

$$R_{\mathrm{com}} \approx \frac{\mathbf{w}_{\mathrm{com}}^H\mathbf{H}_{\mathrm{com}}\mathbf{F}_{\mathrm{RF}}^{\mathrm{com}}\mathbf{S}\mathbf{F}_{\mathrm{BB}}^{\mathrm{com}}\mathbf{F}_{\mathrm{BB}}^{\mathrm{com}H}\mathbf{S}\mathbf{F}_{\mathrm{RF}}^{\mathrm{com}H}\mathbf{H}_{\mathrm{com}}^H\mathbf{w}_{\mathrm{com}}}{\sigma_{\mathrm{rad-com}}^2 + \zeta_{\mathrm{com}}^2}, \tag{14}$$

where the numerator can be written as:

$$\begin{aligned}\rho_{\mathrm{com}} &\triangleq \mathbf{w}_{\mathrm{com}}^H\mathbf{H}_{\mathrm{com}}\mathbf{F}_{\mathrm{RF}}^{\mathrm{com}}\mathbf{S}\mathbf{F}_{\mathrm{BB}}^{\mathrm{com}}\mathbf{F}_{\mathrm{BB}}^{\mathrm{com}H}\mathbf{S}\mathbf{F}_{\mathrm{RF}}^{\mathrm{com}H}\mathbf{H}_{\mathrm{com}}^H\mathbf{w}_{\mathrm{com}} \\ &= \mathbf{w}_{\mathrm{com}}^H\mathbf{H}_{\mathrm{com}}\mathbf{F}_{\mathrm{RF}}^{\mathrm{com}}\mathbf{S}\mathbf{F}_{\mathrm{RF}}^{\mathrm{com}H}\mathbf{H}_{\mathrm{com}}^H\mathbf{w}_{\mathrm{com}},\end{aligned} \tag{15}$$

given that $\mathbf{F}_{\mathrm{BB}}^{\mathrm{com}}\mathbf{F}_{\mathrm{BB}}^{\mathrm{com}H} = \mathbf{I}$ and $\mathbf{S}$ is an idempotent matrix, that is, $\mathbf{SS} = \mathbf{S}$. The denominator $\sigma_{\mathrm{rad-com}}^2$ is given by:

$$\begin{aligned}\sigma_{\mathrm{rad-com}}^2 = \mathbb{E}\Big\{&\left(\mathbf{w}_{\mathrm{com}}^H\mathbf{H}_{\mathrm{com}}\left(\mathbf{F}_{\mathrm{RF}}^{\mathrm{rad}}\mathbf{S}\mathbf{F}_{\mathrm{BB}}^{\mathrm{rad}}\mathbf{s}_{\mathrm{rad}} + \mathbf{F}_{\mathrm{RF}}^{\mathrm{com}}\mathbf{S}\mathbf{F}_{\mathrm{BB}}^{\mathrm{rad}}\mathbf{s}_{\mathrm{rad}}\right.\right. \\ &\left.\left. + \mathbf{F}_{\mathrm{RF}}^{\mathrm{rad}}\mathbf{S}\mathbf{F}_{\mathrm{BB}}^{\mathrm{com}}\mathbf{s}_{\mathrm{com}}\right) + n\right)\left(\mathbf{w}_{\mathrm{com}}^H\mathbf{H}_{\mathrm{com}}\left(\mathbf{F}_{\mathrm{RF}}^{\mathrm{rad}}\mathbf{S}\mathbf{F}_{\mathrm{BB}}^{\mathrm{rad}}\mathbf{s}_{\mathrm{rad}}\right.\right. \\ &\left.\left. + \mathbf{F}_{\mathrm{RF}}^{\mathrm{com}}\mathbf{S}\mathbf{F}_{\mathrm{BB}}^{\mathrm{rad}}\mathbf{s}_{\mathrm{rad}} + \mathbf{F}_{\mathrm{RF}}^{\mathrm{rad}}\mathbf{S}\mathbf{F}_{\mathrm{BB}}^{\mathrm{com}}\mathbf{s}_{\mathrm{com}}\right) + n\right)^H\Big\}\end{aligned} \tag{16}$$

$$\begin{aligned}&= 2\mathbf{w}_{\mathrm{com}}^H\mathbf{H}_{\mathrm{com}}\mathbf{F}_{\mathrm{RF}}^{\mathrm{rad}}\mathbf{S}\left(\mathbf{w}_{\mathrm{com}}^H\mathbf{H}_{\mathrm{com}}\mathbf{F}_{\mathrm{RF}}^{\mathrm{rad}}\right)^H \\ &\quad + \mathbf{w}_{\mathrm{com}}^H\mathbf{H}_{\mathrm{com}}\mathbf{F}_{\mathrm{RF}}^{\mathrm{com}}\left(\mathbf{w}_{\mathrm{com}}^H\mathbf{H}_{\mathrm{com}}\mathbf{F}_{\mathrm{RF}}^{\mathrm{com}}\right)^H + \sigma_n^2 \\ &= 2\mathbf{w}_{\mathrm{com}}^H\mathbf{H}_{\mathrm{com}}\mathbf{F}_{\mathrm{RF}}^{\mathrm{rad}}\mathbf{S}^{(i)}\left(\mathbf{F}_{\mathrm{RF}}^{\mathrm{rad}}\right)^H\mathbf{H}_{\mathrm{com}}^H\mathbf{w}_{\mathrm{com}} \\ &\quad + \mathbf{w}_{\mathrm{com}}^H\mathbf{H}_{\mathrm{com}}\mathbf{F}_{\mathrm{RF}}^{\mathrm{com}}\mathbf{S}^{(i)}\mathbf{F}_{\mathrm{RF}}^{\mathrm{com}}\mathbf{H}_{\mathrm{com}}^H\mathbf{w}_{\mathrm{com}} + \sigma_n^2,\end{aligned} \tag{17}$$

given that $\mathbb{E}\{\mathbf{s}_{\mathrm{com}}\mathbf{s}_{\mathrm{com}}^H\} = \mathbf{I}$. For ζ_{com}^2, we have that

$$\zeta_{\mathrm{com}}^2 = \mathbf{w}_{\mathrm{com}}^H\mathbf{H}_{\mathrm{com}}\mathbf{\Phi}\mathbf{\Phi}^H\mathbf{H}_{\mathrm{com}}^H\mathbf{w}_{\mathrm{com}}. \tag{18}$$

Similarly for the radar operation, we can write the radar rate expression as

$$R_{\mathrm{rad}} \approx \frac{\mathbf{w}_{\mathrm{rad}}^H\mathbf{H}_{\mathrm{rad}}\mathbf{F}_{\mathrm{RF}}^{\mathrm{rad}}\mathbf{S}\mathbf{F}_{\mathrm{BB}}^{\mathrm{rad}}\mathbf{F}_{\mathrm{BB}}^{\mathrm{rad}H}\mathbf{S}\mathbf{F}_{\mathrm{RF}}^{\mathrm{rad}H}\mathbf{H}_{\mathrm{rad}}^H\mathbf{w}_{\mathrm{rad}}}{\sigma_{\mathrm{com-rad}}^2 + \zeta_{\mathrm{rad}}^2}, \tag{19}$$

where the numerator can be written as

$$\rho_{\text{rad}} \triangleq \mathbf{w}_{\text{rad}}^H \mathbf{H}_{\text{rad}} \mathbf{F}_{\text{RF}}^{\text{rad}} \mathbf{S} \mathbf{F}_{\text{BB}}^{\text{rad}} \mathbf{F}_{\text{BB}}^{\text{rad}H} \mathbf{S} \mathbf{F}_{\text{RF}}^{\text{rad}H} \mathbf{H}_{\text{rad}}^H \mathbf{w}_{\text{rad}} = \mathbf{w}_{\text{rad}}^H \mathbf{H}_{\text{rad}} \mathbf{F}_{\text{RF}}^{\text{rad}} \mathbf{S} \mathbf{F}_{\text{RF}}^{\text{rad}H} \mathbf{H}_{\text{rad}}^H \mathbf{w}_{\text{rad}}, \tag{20}$$

given that $\mathbf{F}_{\text{BB}}^{\text{rad}} \mathbf{F}_{\text{BB}}^{\text{rad}H} = \mathbf{I}$. Similarly for a given $\mathbb{E}\{\mathbf{s}_{\text{rad}} \mathbf{s}_{\text{rad}}^H\} = \mathbf{I}$, following above, we can write the denominator term $\sigma_{\text{com-rad}}^2$ of the radar rate expression as follows:

$$\sigma_{\text{com-rad}}^2 = 2\mathbf{w}_{\text{rad}}^H \mathbf{H}_{\text{rad}} \mathbf{F}_{\text{RF}}^{\text{com}} \mathbf{S}^{(i)} \left(\mathbf{F}_{\text{RF}}^{\text{com}}\right)^H \mathbf{H}_{\text{rad}}^H \mathbf{w}_{\text{rad}} + \mathbf{w}_{\text{rad}}^H \mathbf{H}_{\text{rad}} \mathbf{F}_{\text{RF}}^{\text{rad}} \mathbf{S}^{(i)} \mathbf{F}_{\text{RF}}^{\text{rad}H} \mathbf{H}_{\text{rad}}^H \mathbf{w}_{\text{rad}} + \sigma_n^2, \tag{21}$$

and

$$\zeta_{\text{rad}}^2 = \mathbf{w}_{\text{rad}}^H \mathbf{H}_{\text{rad}} \mathbf{\Phi} \mathbf{\Phi}^H \mathbf{H}_{\text{rad}}^H \mathbf{w}_{\text{rad}}. \tag{22}$$

3.2 | Fractional programing

From Equations (14) and (19), it is obvious that the approximated cost function is fractional. Specifically, for the communications case,

$$\max_{\mathbf{S}} \frac{\rho_{\text{com}}(\mathbf{S})}{\sigma_{\text{rad-com}}^2 + \zeta_{\text{com}}^2} \text{ s.t. } \quad \text{tr}\left(\mathbf{F}_{\text{RF}}^{\text{com}} \mathbf{F}_{\text{BB}}^{\text{com}} \mathbf{F}_{\text{BB}}^{\text{com}H} \mathbf{F}_{\text{RF}}^{\text{com}H}\right) \le P_{\text{max}}^{\text{com}}. \tag{23}$$

To deal with a fractional cost function, we employ Dinkelbach (DB) iterations [39], where one iteration of the DB method solves the following problem:

$$\max_{\mathbf{S}} \left\{\rho_{\text{com}}(\mathbf{S}) - \kappa^{(i)} \sigma_{\text{rad-com}}(\mathbf{S})\right\} \text{s.t.} \quad [\mathbf{S}]_{k,k} \in [0,1], \tag{24}$$

for $i = 1, 2, \ldots, I_{\max}$, where

$$\kappa^{(i)} = \rho_{\text{com}}^{(i-1)} / \sigma_{\text{rad-com}}^{(i-1)}, \tag{25}$$

with $\kappa^{(0)} = 1$. The details of the proposed algorithm that solves (24) are shown in Algorithm 1.

Following the same procedure, the maximisation radar rate is expressed as

$$\max_{\mathbf{S}} \left\{\rho_{\text{rad}}(\mathbf{S}) - \kappa^{(i)} \sigma_{\text{com-rad}}(\mathbf{S})\right\} \text{s.t.} \quad [\mathbf{S}]_{k,k} \in [0,1], \tag{26}$$

where similarly, the parameter $\kappa^{(i)}$ is defined at the previous iteration [40], that is,

$$\kappa^{(i)} = \rho_{\text{rad}}^{(i-1)} / \sigma_{\text{com-rad}}^{(i-1)}, \tag{27}$$

with $\kappa^{(0)} = 1$. Equation (26) is solved by Algorithm 2 that describes the proposed RF selection procedure for the radar operation. Next, we present the simulation results to evaluate the effectiveness of the proposed RF selection method for both communication and radar operations for different parameter settings.

Algorithm 2 Proposed RF Selection for Radar Operation

Input: $\mathbf{H}_{\text{com}}$, $\mathbf{H}_{\text{rad}}$
Output: Diagonal binary matrix $\mathbf{S}^{(I_{\max})}$
Set $\kappa^{(0)} = 1$.
for $i = 1, 2, \ldots, I_{\max}$ **do**
  $\kappa^{(i)} = \rho_{\text{rad}}^{(i-1)} / \sigma_{\text{com-rad}}^{(i-1)}$
  Use CVX [41] to solve $\max_{\mathbf{S}} \{\rho_{\text{rad}}(\mathbf{S}) - \kappa^{(i)} \sigma_{\text{com-rad}}\}$ s.t. $[\mathbf{S}]_{k,k} \in [0,1]$
  where R_{rad} is approximated using Equation (19), and $\sigma_{\text{com-rad}}^2$ is given in Equation (21).
  Approximate $R_{\text{rad}}(\mathbf{S}^{(i)})$ via Equation (19).
  Calculate the interference term $\sigma_{\text{com-rad}}^2(\mathbf{S}^{(i)})$ in Equation (21).
  Compute $\kappa^{(i)} = \rho_{\text{rad}}(\mathbf{S}^{(i)}) / \sigma_{\text{com-rad}}^2(\mathbf{S}^{(i)})$.
end for

4 | SIMULATION RESULTS

In this section, we present the numerical results to investigate the performance of the proposed method and its comparison with existing baseline methods. We use MATLAB™ computer simulation results to evaluate the performance curves. All the results are averaged over 500 Monte-Carlo realisations. Let us first define the parameters and the system characteristics. We assume that the TX employs hybrid transmit beamforming with N_{T} antennas, while the number of RF chains is $L_{\text{T}} \le N_{\text{T}}$. Each transmission broadcasts a zero-mean random Gaussian vector with $\mathbf{s} \in \mathbb{C}^{N_{\text{R}} \times 1}$ and $\mathbb{E}\{\mathbf{s}\mathbf{s}^H\} = \mathbf{I}_{N_{\text{R}}}$. We assume ULAs at both TX and UE sides and operating over a 28 GHz outdoor mmWave channel [42]. To focus on the TX performance, we assume digital combining is performed at the UE, that is, $\mathbf{w}_k$ is defined as the k^{th} column of the left orthonormal matrix, obtained by the singular value decomposition of the channel matrix $\mathbf{H}$. Default channel parameter settings are shown in Table 2. Besides, there are three targets for detection operation, where the angular target locations are chosen randomly for each realisation.

Baseline Methods: We consider the following baseline JRC MIMO beamforming (BF) architectures for comparison with the proposed method:

a). Digital BF: This baseline method considers the conventional fully digital beamforming based MIMO JRC architecture with ideal rate performance, where the number of RF chains are same as the number of TX antennas, that is, $L_{\text{T}} = N_{\text{T}}$, such as presented in the

literature for comparison of hybrid beamforming architectures [12, 13].

b). *Digital BF with communication/radar interference*: This baseline method considers a fully digital architecture with the impact of communication or radar interference on the digital precoder. The communication interference occurs when radar operation takes place and vice-versa. The number of RF chains are fixed and equal to the number of TX antennas.

c). *Digital BF with communication/radar interference and hardware impairments*: This baseline method adds up the impact of hardware impairments on the digital precoder in addition to the communication or radar interference. Similar to the above baseline, the radar interference occurs when communication operation takes place and vice-versa. Also there are a fixed number of RF chains equal to the number of TX antennas, that is, $L_T = N_T$.

TABLE 2 Simulation parameter terms and values

Parameter	Value
Carrier frequency	28 GHz
System bandwidth	100 MHz
Delay spread	10 ns
Angle spread	10°
TX Antennas N_T	32
UE Antennas N_R	8
Fading type	Rayleigh fading
Number of subpaths N_m	Random per user;$\mathcal{U}(0, 15)$

d). *Hybrid BF with communication/radar interference and hardware impairments*: This baseline method considers the hybrid beamforming architecture, where the number of RF chains are fewer than the number of TX antennas. In this case, the impact of communication or radar interference and hardware impairments on the hybrid precoder is also taken into account. The interference term is dependent on which operation out of the two takes place, that is, the radar interference occurs when communication operation takes place and vice-versa.

Proposed RF Selection Method:

e). *Proposed method with communication/radar interference and hardware impairments*: The proposed method considers hybrid precoding architecture with the impact of communication or radar interference and hardware impairments and with optimal number of RF chains unlike the fixed RF chain cases of the baseline methods. In the scope of this paper, we present optimal RF selection mechanism with hardware impairments and interference terms taken into account, similar fractional programing-based RF chain selection procedures can also be extended with DAC-bit selection in JRC systems such as in Ref. [43].

Convergence Analysis: In Figure 2, we present the convergence curve of the proposed method for different signal-to-noise ratio (SNR) values. The parameter κ is observed against the iteration index in the proposed algorithm, and the convergence performance is checked for different SNR values. It can be observed that after 3–4 iterations, the proposed DB solution converges, resulting in an efficient approach for RF selection in MIMO JRC systems.

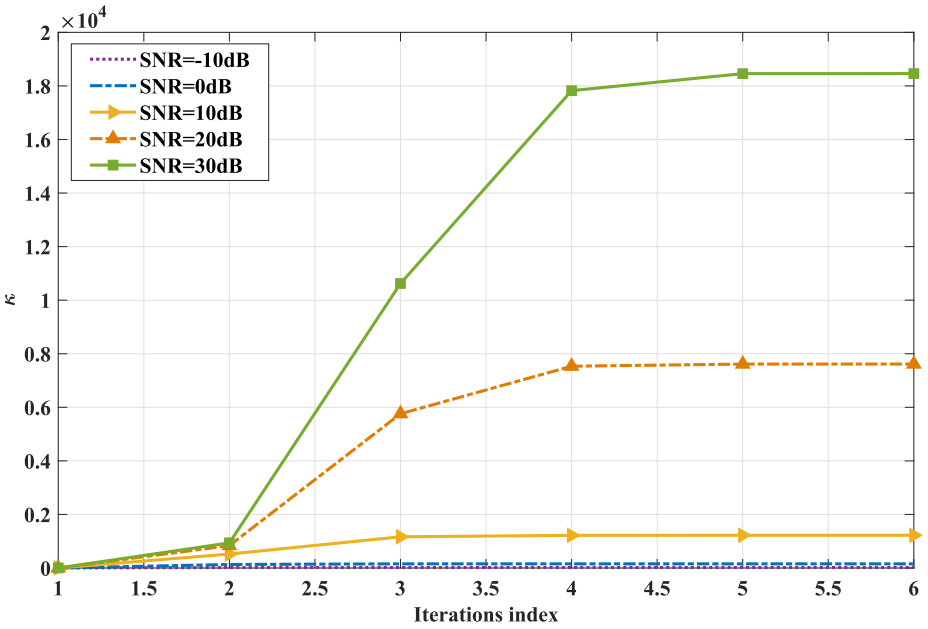

FIGURE 2 Convergence curve of the proposed method

Communication Performance: In Figure 3, we present the communication rate performance versus SNR for the proposed method and compare it with the above mentioned baseline methods. It can be observed that the proposed RF chain selection method outperforms baseline approaches (b)–(d) and performs close to the ideal fully digital beamforming method, especially at low SNR values. For example, at 30 dB SNR, the proposed RF chain selection method with hybrid beamforming outperforms the baseline methods with a fixed number of RF chains, which are the hybrid BF (with radar interference and hardware impairments), the digital BF (with radar interference and hardware impairments) and the digital BF with radar interference by ≈4 Mbits/s, ≈3 Mbits/s and ≈1 Mbits/s, respectively.

In Figures 4 and 5, we evaluate the communication rate performance of different algorithms with respect to variation in noise variance of the hardware impairments and the total number of available RF chains, respectively. In Figure 4, it can be observed that the proposed method outperforms baseline methods (c) and (d) when the impact of hardware impairments is considered. When the noise variance is 0.1, the proposed RF selection method outperforms baseline methods (c) and (d)

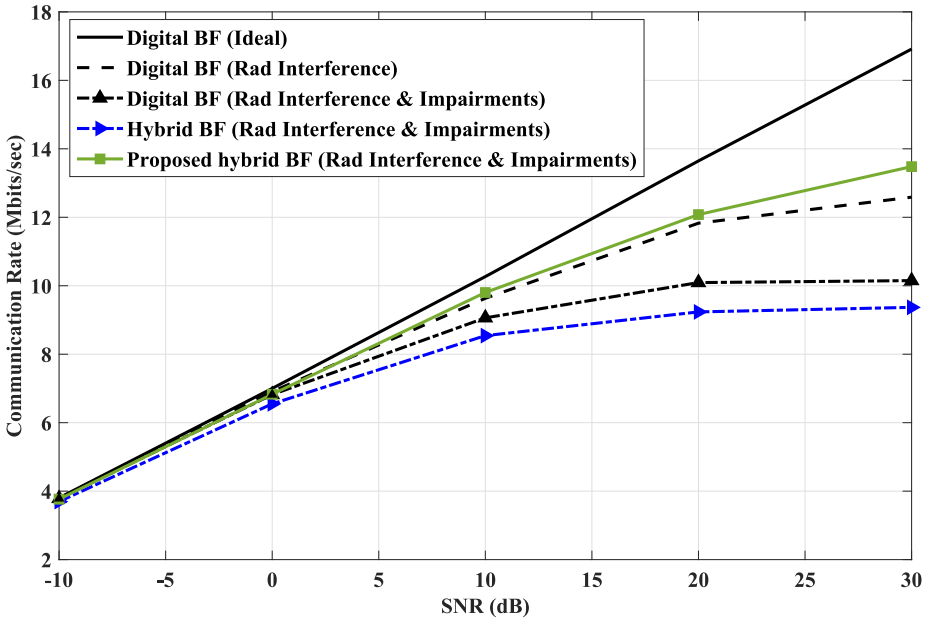

FIGURE 3 Communication rate versus signal-to-noise ratio (SNR), $N_T = 32$ and $N_R = 8$

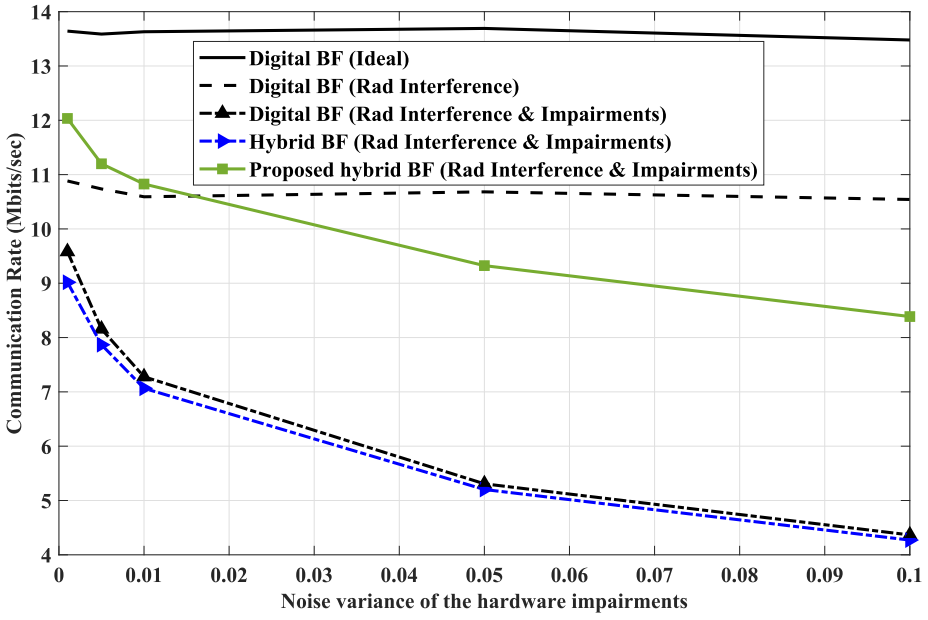

FIGURE 4 Communication rate versus hardware impairments noise variance, $N_T = 32$ and $N_R = 8$

by ≈4 Mbits/s and ≈3.9 Mbits/s, respectively. Similarly, in Figure 5, it can be observed that the proposed RF selection method outperforms the baseline methods (b), (c) and (d), which use a fixed number of RF chains, in terms of the communication rate. The optimal number of RF chains out of the total available number of RF chains often results into $L_{\mathrm{T}}^{opt} = 2$ as shown in Figure 5.

Radar Performance: For the MIMO JRC system, we also observe the radar rate performance with respect to variations in SNR, hardware impairments noise variance, and the number of available RF chains in Figures 6–8, respectively. It can be observed from Figure 6 that the proposed RF selection method with hybrid beamforming outperforms the baseline methods in (b)–(d) and exhibits close performance to the digital BF (ideal) in the low SNR region. Note that for the radar operation, the impact of communication interference and hardware impairments is considered. For example, at 30 dB SNR, the proposed method performs ≈3.5 Mbits/s better than the baselines (b)–(c) and ≈4.5 Mbits/sec better than the baseline (d) using hybrid beamforming with a fixed number of RF chains and considering the impact of communication interference and hardware impairments.

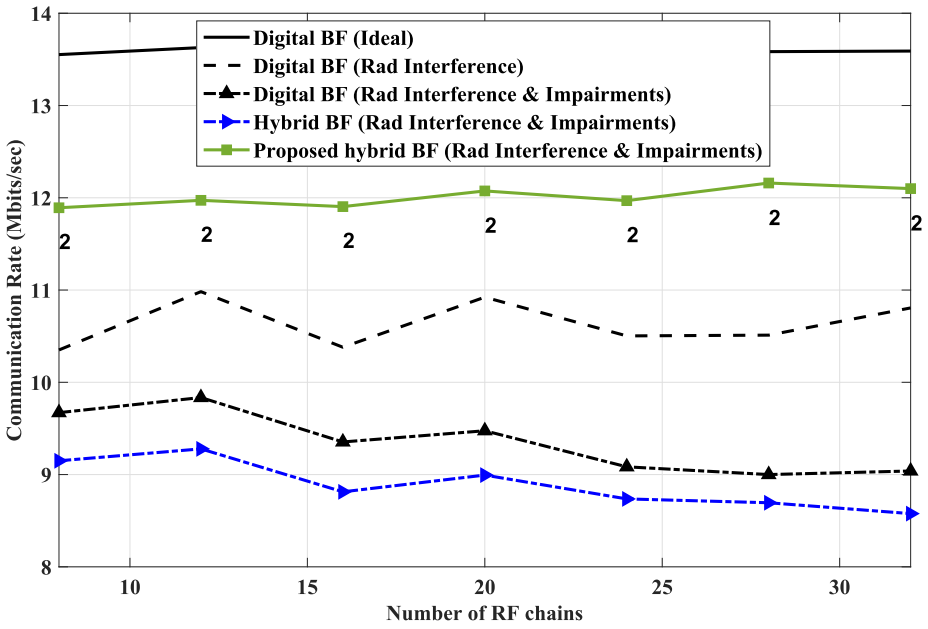

FIGURE 5 Average number of selected radio frequency (RF) chains for the proposed method and communication rate performance, $N_{\mathrm{T}} = 32$ and $N_{\mathrm{R}} = 8$

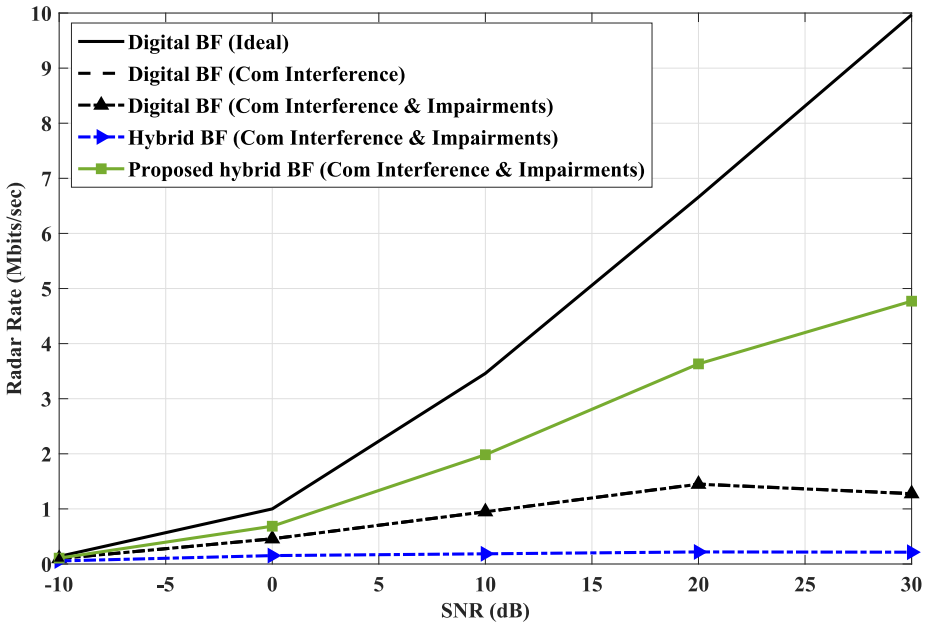

FIGURE 6 Radar rate versus signal-to-noise ratio (SNR), $N_{\mathrm{T}} = 32$ and $N_{\mathrm{R}} = 8$

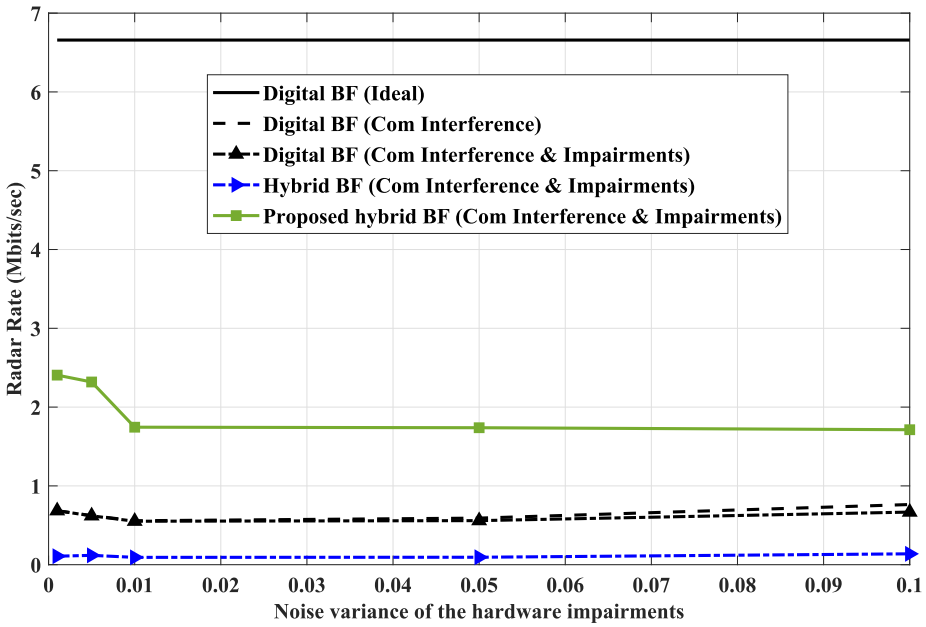

FIGURE 7 Radar rate versus hardware impairments noise variance, $N_T = 32$ and $N_R = 8$

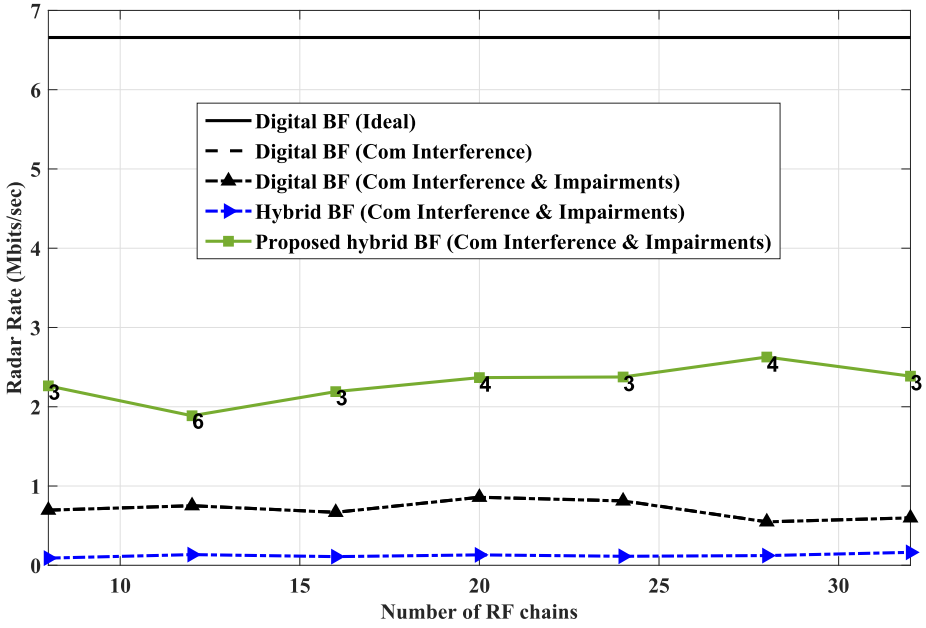

FIGURE 8 Average number of selected radio frequency (RF) chains for the proposed method and radar rate performance, $N_T = 32$ and $N_R = 8$

Similarly, in Figure 7, the radar rate of the proposed RF selection case shows better performance than the baseline methods in (b)–(d). In Figure 8, again it can be observed that, the proposed method outperforms the baseline methods in (b)–(d) when the number of available RF chains varies. The optimal number of RF chains in the proposed method comes often as $L_T^{opt} = 3$ or $L_T^{opt} = 4$ as can be observed from Figure 8. We can infer that out of the available number of RF chains, the proposed method while choosing fewer number of RF chains enhances the cost efficiency and hence lowers power consumption. In addition the proposed RF selection method also exhibits good spectral efficiency performance outperforming the standard baseline methods.

Communication-Radar Trade-off: We also measure the trade-off between the communication rate and radar rate performance for the proposed approach and different baseline algorithms. In Figure 9, the variation of communication rate against radar rate in the scale of Mbits/sec can be observed for different method. For example, when the communication rate is ≈12 Mbits/sec, the radar rate is ≈4 Mbits/sec for the proposed RF selection scenario. However, the baseline

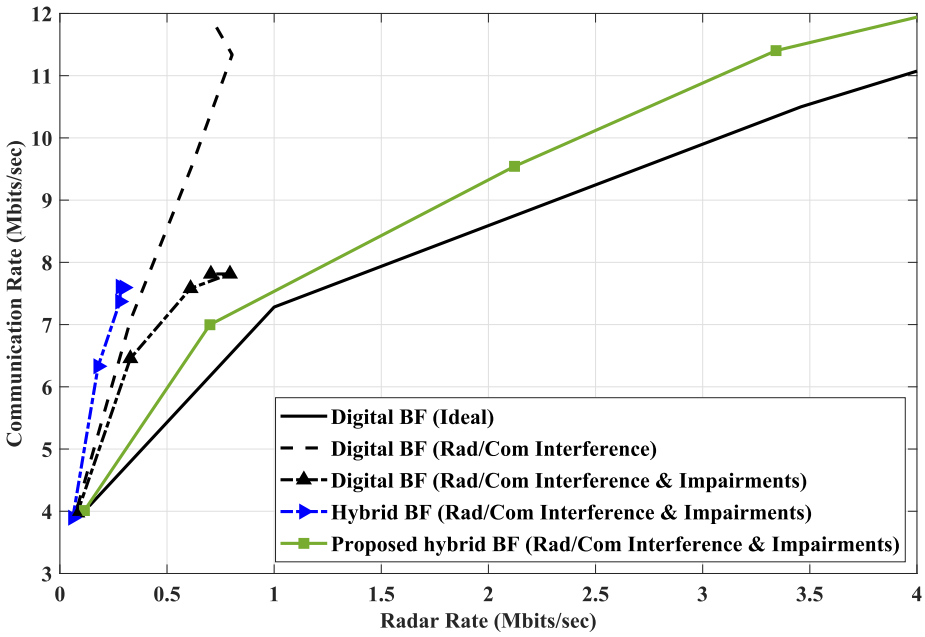

FIGURE 9 Communication rate versus radar rate performance trade-off, $N_T = 32$ and $N_R = 8$

algorithms in (b)–(d) with a fixed number of RF chains are not able to achieve such high spectral efficiency performance gains as the proposed RF selection method.

5 | CONCLUSION

This paper presents a spectrally efficient method for MIMO JRC systems with hybrid beamforming architecture. It selects the optimal number of RF chains while the impact of communication/radar interference and hardware impairments is taken into account. Implicitly, selecting only the required number of RF chains for each channel realisation also enhances the cost efficiency of integrated JRC systems. The proposed method outperforms the baseline methods both in terms of communication and radar rate values with respect to variations in different signalling and system parameters. The impact of interference of one operation to the other and hardware impairment error on the performance of the proposed method and baseline approaches is also observed. For instance, at 30 dB SNR, the proposed RF selection method increases the communication rate performance by ≈40% and the radar rate performance by ≈ 45% when compared with the hybrid beamforming baseline with fixed number of RF chains while also considering the impact of radar interference and hardware impairments. Future work will include the energy efficiency maximisation via the RF chain selection procedure in MIMO JRC systems with hybrid beamforming and low resolution DAC-based architecture.

ACKNOWLEDGMENTS

The corresponding author's institution has an existing agreement with Wiley which will pay (or have paid) the Article Publication Charge on behalf of the author.

This work was supported by the Engineering and Physical Sciences Research Council Grant number EP/S000631/1 and the MOD University Defence Research Collaboration in Signal Processing. The authors would also like to acknowledge the support of the School of Engineering and Informatics, University of Sussex.

CONFLICT OF INTEREST

There is no conflict of interest to disclose by the authors.

DATA AVAILABILITY STATEMENT

Data available on request from the authors.

ORCID

Aryan Kaushik https://orcid.org/0000-0001-6252-4641

REFERENCES

1. Cisco annual internet report 2018-23 white paper. (2020). https://www.cisco.com/c/en/us/solutions/collateral/executive-perspectives/annual-internet-report/white-paper-c11-741490.html
2. Ericsson mobility report. 1–40 (2021). https://www.ericsson.com/4ad7e9/assets/local/reports-papers/mobility-report/documents/2021/ericsson-mobility-report-november-2021.pdf
3. 5G Americas white paper: mobile communications towards 2030. 1–56 (2021). https://www.5gamericas.org/wp-content/uploads/2021/11/Mob-Comm-Towards-2030-WP.pdf
4. Griffiths, H., et al.: Radar spectrum engineering and management: technical and regulatory issues. Proc. IEEE. 103(1), 85–102 (2015)
5. Paul, B., Chiriyath, A.R., Bliss, D.W.: Survey of RF communications and sensing convergence research. IEEE Access. 5, 252–270 (2017)
6. Liu, F., et al.: Joint radar and communication designs: applications, state-of-the-art, and the road ahead. IEEE Trans. Commun. 68(6), 3834–3862 (2020)
7. Cui, Y., et al.: Integrating sensing and communications for ubiquitous IoT: applications, trends and challenges. arXiv2104.11457 (2021)

8. Tavik, G.C., et al.: The advanced multifunction RF concept. IEEE Trans. Microw. Theor. Tech. 53(3), 1009–1020 (2005)
9. Sturm, C., Wiesbeck, W.: Waveform design and signal processing aspects for fusion of wireless communications and radar sensing. Proc. IEEE. 99(7), 1236–1259 (2011)
10. Zhang, J.A., et al.: An overview of signal processing techniques for joint communication and radar sensing. IEEE J. Sel. T. Sig. P., in press
11. Chen, S., et al.: Pre-scaling and codebook design for joint radar and communication based on index modulation. arXiv:2111.10527, 1–4 (2021)
12. Kaushik, A., et al.: Sparse hybrid precoding and combining in millimeter wave MIMO systems. IET Radio Propagation Technol. 1–7 (2016)
13. Vlachos, E., et al.: Radio-frequency chain selection for energy and spectral efficiency maximisation in hybrid beamforming under hardware imperfections. Proc. Royal Soc. A. 476(2244), 1–20 (2020)
14. Wymeersch, H., et al.: 5G mmWave positioning for vehicular networks. IEEE Wireless Commun. 24(6), 80–86 (2017)
15. Zhang, J.A., et al.: Multibeam for joint communication and radar sensing using steerable analogue antenna arrays. IEEE Trans. Veh. Technol. 68(1), 671–685 (2019)
16. Dokhanchi, S.H., et al.: A mmWave automotive joint radar-communications system. IEEE Trans. Aero. Electron. Syst. 55(3), 1241–1260 (2019)
17. Mishra, K.V., et al.: Toward millimetre-wave joint radar communications: a signal processing perspective. IEEE Signal Process. Mag. 36(5), 100–114 (2019)
18. Cui, Y., et al.: Interference alignment based spectrum sharing for MIMO radar and communication systems. IEEE Int. Workshop Sig. Process. Adv. Wireless Commun. (SPAWC), 1–5 (2018)
19. Liu, F., et al.: MIMO radar and cellular coexistence: a power-efficient approach enabled by interference exploitation. IEEE Trans. Signal Process. 66(14), 3681–3695 (2018)
20. Liu, F., et al.: MU-MIMO communications with MIMO radar: from co-existence to joint transmission. IEEE Trans. Wireless Commun. 17(4), 2755–2770 (2018)
21. Kaushik, A., et al.: Waveform design for joint-radar communications with low complexity analogue components. IEEE Int. Symposium Joint Comms. Sensing. 1–5 (2022)
22. Kaushik, A., et al.: Dynamic RF chain selection for energy efficient and low complexity hybrid beamforming in millimetre wave MIMO systems. IEEE Trans. Green Commun. Netw. 3(4), 886–900 (2019)
23. Kaushik, A., et al.: Energy efficiency maximisation in millimetre wave hybrid MIMO systems for 5G and beyond. IEEE Int. Conf. Commun. Netw. (ComNet), 1–7 (2020)
24. Molisch, A.F., et al.: Hybrid beamforming for massive MIMO: a survey. IEEE Commun. Mag. 55(9), 134–141 (2017)
25. Kaushik, A., et al.: Hardware efficient joint radar-communications with hybrid precoding and RF chain optimisation. IEEE Int. Conf. Commun. 1–6 (2021)
26. Walden, R.H.: Analogue-to-digital converter survey and analysis. IEEE J. Sel. Area. Commun. 17(4), 539–550 (1999)
27. Kaushik, A., et al.: Efficient channel estimation in millimetre wave hybrid MIMO systems with low resolution ADCs. IEEE European Sig. Process. Conf. 1825–1829 (2018)
28. Kaushik, A., et al.: Energy efficient ADC bit allocation and hybrid combining for millimetre wave MIMO systems. IEEE Global Commun. Conf., HI, USA, 1–6 (2019)
29. Kumari, P., et al.: A low-resolution ADC proof-of-concept development for a fully-digital millimetre-wave joint communication-radar. Proc. IEEE Int. Conf. Acous. Speech Sig. Process. (ICASSP), 8619–8623 (2020)
30. Kaushik, A., et al.: Energy efficiency maximisation of millimetre wave hybrid MIMO systems with low resolution DACs. IEEE Int. Conf. Commun., 1–6 (2019)
31. Kaushik, A., et al.: Joint bit allocation and hybrid beamforming optimisation for energy efficient millimetre wave MIMO systems. IEEE Trans. Green Commun. Netw. 5(1), 119–132 (2021)
32. Dizdar, O., et al.: Rate-splitting multiple access for joint radar-communications with low-resolution DACs. IEEE Int. Conf. Commun. (ICC) Workshop, 1–6 (2021)
33. Kaushik, A. et al.: Green joint radar-communications: RF selection with low resolution DACs and hybrid precoding. IEEE Int. Conf. Commun. 1–6 (2022)
34. Yang, X., et al.: Hardware-constrained millimetre-wave systems for 5G: challenges, opportunities, and solutions. IEEE Commun. Mag. 57(1), 44–50 (2019)
35. Tang, B., Li, J.: Spectrally constrained MIMO radar waveform design based on mutual information. IEEE Trans. Signal Process. 67(3), 821–834 (2019)
36. Xu, R., et al.: Radar mutual information and communication channel capacity of integrated radar-communication system using MIMO. ICT Express. 1(3), 102–105 (2015)
37. Yang, Y., Blum, R.S.: MIMO radar waveform design based on mutual information and minimum mean-square error estimation. IEEE Trans. Aero. Electron. Syst. 1–12 (2007)
38. Bica, M., et al.: Mutual information based radar waveform design for joint radar and cellular communication systems. IEEE Int. Conf. Acoustics, Speech Sig. Process. (ICASSP), 3671–3675 (2016)
39. Crouzeix, J.-P., Ferland, J.A.: Algorithms for generalised fractional programming. Mathematical Programming, Springer-Verlag. 52(1–3), 191–207 (1991)
40. Zappone, A., Jorswieck, E.: Energy efficiency in wireless networks via fractional programming theory. Found. Trends™ Commun. Inf. Theory. 11(3–4), 185–396 (2015)
41. Grant, M., Boyd, S.: CVX: matlab software for disciplined convex programming. Version 2.1 (2014)
42. Forenza, A., Love, D.J., Heath, R.W.: Simplified spatial correlation models for clustered MIMO channels with different array configurations. IEEE Trans. Veh. Technol. 564, 1924–1934 (2007)
43. Dizdar, O., et al.: Energy efficient dual-functional radar-communication: rate-splitting multiple access, low-resolution DACs, and RF chain selection. arXiv:2202.09128, 1–17 (2022)

How to cite this article: Kaushik, A., et al.: Towards 6G: spectrally efficient joint radar and communication with radio frequency selection, interference and hardware impairments (invited paper). IET Signal Process. 16(7), 851–863 (2022). https://doi.org/10.1049/sil2.12131